



HHS Public Access

Author manuscript

Bioorg Med Chem Lett. Author manuscript; available in PMC 2018 May 01.

Published in final edited form as:

Bioorg Med Chem Lett. 2017 May 01; 27(9): 2029–2037. doi:10.1016/j.bmcl.2017.02.068.

High-content screen using Zebrafish (*Danio rerio*) embryos identifies a novel kinase activator and inhibitor

Werner J. Geldenhuis^{a,*}, Sadie A. Bergeron^b, Jackie E. Mullins^b, Rowaa Aljammal^a, Briah L. Gaasch^a, Wei-Chi Chen^a, June Yun^c, and Lori A. Hazlehurst^a

^aDepartment of Pharmaceutical Sciences, School of Pharmacy, West Virginia University, Morgantown, WV 26506

^bDepartment of Biology, Eberly College of Arts and Sciences, West Virginia University, Morgantown WV 26506

^cDepartment of Integrative Medical Sciences, College of Medicine, Northeast Ohio Medical University, Rootstown OH 44272

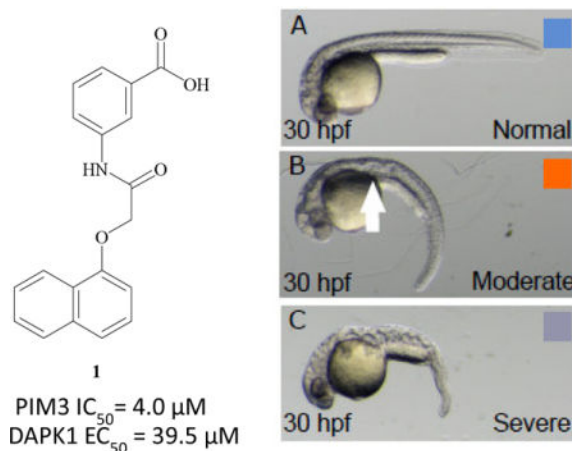
Abstract

In this report we utilized zebrafish (*Danio rerio*) embryos in a phenotypical high-content screen (HCS) to identify novel leads in a cancer drug discovery program. We initially validated our HCS model using the flavin adenosine dinucleotide (FAD) containing endoplasmic reticulum (ER) enzyme, endoplasmic reticulum oxidoreductase (ERO1) inhibitor EN460. EN460 showed a dose response effect on the embryos with a dose of 10 μ M being significantly lethal during early embryonic development. The HCS campaign which employed a small library identified a promising lead compound, a naphthyl-benzoic acid derivative coined compound 1 which had significant dosage and temporally dependent effects on notochord and muscle development in zebrafish embryos. Screening a 369 kinase member panel we show that compound 1 is a PIM3 kinase inhibitor ($IC_{50} = 4.078 \mu$ M) and surprisingly a DAPK1 kinase agonist/activator ($EC_{50} = 39.525 \mu$ M). To our knowledge this is the first example of a small molecule activating DAPK1 kinase. We provide a putative model for increased phosphate transfer in the ATP binding domain when compound 1 is virtually docked with DAPK1. Our data indicate that observable phenotypical changes can be used in future zebrafish screens to identify compounds acting via similar molecular signaling pathways.

TOC image

*Corresponding author: 1 Medical Center Drive, Morgantown WV 26506; werner.geldenhuis@hsc.wvu.edu.

Publisher's Disclaimer: This is a PDF file of an unedited manuscript that has been accepted for publication. As a service to our customers we are providing this early version of the manuscript. The manuscript will undergo copyediting, typesetting, and review of the resulting proof before it is published in its final citable form. Please note that during the production process errors may be discovered which could affect the content, and all legal disclaimers that apply to the journal pertain.



Keywords

phenotypic screen; cancer; zebrafish; kinase; compound library; notochord; somites

Cancer is a complex disease group with more than 100 specific subtypes. There are more than a million new cancer patients estimated in 2016.¹ To identify novel molecular targets and develop oncology therapeutics remains an important goal to adequately and successfully treat cancer patients.² One approach to identify novel drugable targets is the use of high content phenotypic screens using whole organisms.³ The use of whole organism screens naturally selects for compounds which have a profile that is drug-like in nature, with intrinsic pharmacokinetic and toxicological effects part of a hit compound. Several of these types of phenotypic screens have been described, including the fruit fly (*Drosophila melanogaster*)⁴ as well as the zebrafish (*Danio rerio*).^{3, 5} Several studies have shown that these organisms can be used for high throughput screening (HTS) and for identifying novel compounds to be used in drug development campaigns. In this study, we screened an in-house compound library of 80 structurally diverse compounds using a zebrafish embryo high content screen (HCS) in a 96-well plate format, to identify novel compounds which may have utility in cancer drug discovery programs.

Compounds were initially screened at 100 μ M and embryos evaluated daily for observable developmental changes using a dissecting microscope. Our library was made up of several compounds from previous studies,^{6, 7} and the compounds were originally obtained from Chembridge (www.hit2lead.com). In this study, we screened 80 compounds which were each representative of a chemotype for which we have additional compound to explore structure-activity relationship studies, latter kept in separate plates. From this screen we visually evaluated each of 96 wells per plate containing a single embryo for changes in phenotype. Our initial criterion were embryotic death (observed as loss of structure), gross deformities, or delayed hatching from egg sack.

A culmination of the results of our HCS validation and testing are shown in figures 1 and 2 respectively. Zebrafish eggs were collected, staged, and placed in 12-well plates with E3 embryo media within the first 6 hours post fertilization (hpf). Tests were done between 6–

30hpf and also after 30hpf. Each well contained 1 mL of E3 media plus 1% DMSO with or without the compound at the initially screened and additional concentrations. No more than 30 embryos were tested per well. As a control compound, we used EN460 to establish the Z-score for this HCS assay. EN460 is an inhibitor of the Flavin adenosine dinucleotide (FAD) containing endoplasmic reticulum (ER) enzyme endoplasmic reticulum oxidoreductase (ERO1). ERO1L is an endoplasmic reticulum resident oxidoreductase which utilizes oxygen and FAD to form denovo disulfide bridges. ERO1L shuttles disulfide bridges to protein disulfide isomerase (PDI) which in turn oxidizes target proteins and contributes to protein folding.⁸ EN460 is reported to inhibit the ERO1L enzyme with an IC₅₀ of 1.9 μM.⁸ Bioinformatics data mining indicated that the ERO1 enzyme is present in zebrafish, however the gene encoding this enzyme was duplicated during teleost evolution (*ero1a*, NM_200350 and *ero1b*, NM_001076638). We wanted to validate this HCS with EN460 so that we could identify novel compounds which interact with proteins *a priori* of knowing the specific target. Secondly, we used a non-kinase inhibitor control compound since it would be informative as to the ability of the assay to identify both kinase inhibitors as well as non-kinase inhibitor compounds which affect other types of cellular organelles such as mitochondria or ER. For example, decoupling of protein folding leads to activation of the unfolded protein response and cell death in cancers that are highly secretory such as Multiple Myeloma.⁹ Critical pathways and targets which regulate the unfolded protein response can be overlooked in a pure kinase screen.

A dose-response assay was done using EN460 ranging from 1–20 μM. Lethal effects were identified at the 10 μM dose, with 5 μM mostly viable through development and successful hatching of the embryos as can be seen in Figure 1. Subsequent assay development suggested the level of solvent DMSO was tolerated up to 5%, and the Z-factor for this assay was >0.9.¹⁰ Our data indicate that ERO1L dependent disulfide bridge formation is critical for proper development of zebrafish suggesting that the zebrafish HCS is a tractable strategy for screening modulators of the ER stress pathway.

Utilizing this assay format, we identified a novel compound from a HCS, compound 1 (7745532) (Figure 2). Zebrafish embryos treated with compound 1 were found to be affected when treated from 6–30 hpf at varying concentrations. The embryos showed increasing morphological changes specifically in the notochord and the tail musculature resulting in a downward c-bend of the body axis. These phenotypical changes were not observable when the eggs were treated at 30 hpf, suggesting the target proteins are active in the first day of development and a low risk of overt toxicity in differentiated tissue. To narrow down the developmental window of time in which compound 1 had the greatest effect, we treated embryos starting at different developmental time points from 6 hpf to 26 hpf. We chose the 100 μM dosage as it showed only a moderate effect on embryonic development from which we could determine changes in phenotypic severity. We saw visible changes to notochord and somite development with treatments from compound 1 at 6 to 14 hpf, however, beyond 22 hpf, no gross morphological phenotype was observed. In addition the tail defects became localized more and more caudally with increasing developmental time suggesting that the targeted kinase is active in newly forming tail musculature or in a rostral to caudal gradient during development.

To identify possible targets with which compound 1 interacts with, we tested compound 1 in a kinase panel (www.reactionbiology.com) since these small molecule inhibitors of kinases are attractive leads for cancer drug discovery.^{11, 12} The panel consisted of 369 wild type kinases which are commonly found to be drug targets in several disease types. Figure 3 shows the results of the panel screen. The two kinases which were chosen from this screen for further exploration were PIM3 and DAPK1 as the two most extreme activities.

Compound 1 was found to inhibit PIM3 kinase with selectivity against PIM1 and PIM2. PIM kinases belong to the Ser/Thr kinase family and have been identified as novel oncology drug targets.¹³ Follow-up with a dose-response study found that compound 1 inhibited PIM3 with an IC₅₀ of 4.078 μ M (figure 4). The control compound for the PIM3 kinase assay was staurosporine, with an inhibition of 0.1206 nM. Additionally, the kinase panel screen showed that compound 1 activated death associated protein kinase 1 (DAPK1). DAPK1 is a Ca²⁺/calmodulin (CaM)-dependent serine/threonine protein kinase which plays a role in autophagy and apoptosis.¹⁴ This was a surprising finding in that compound 1 stimulated/activated DAPK1 in contrast to the inhibition which we would have expected. A dose-response assay indicated that compound 1 is able to stimulate the kinase activity with an EC₅₀ value of 39.525 μ M. The control compound for the DAPK1 kinase assay was staurosporine, with an inhibition of 9.4 nM (Figure 4).

To evaluate the interaction between compound 1 and the two kinases identified from the panel screen, docking studies were done. Since the crystal structure of PIM3 has not been published we developed a homology model of the PIM3 kinase, based on the PIM1 crystal structure using PIM1 (2BZN) as template (Figure 5).¹⁵ We utilized the homology modeling builder function in the program YASARA (www.yasara.com). For the docking study, the PIM3 homology model was prepared for docking in MOE 2016.08 (www.chemcomp.com) by adjusting the hydrogens and charge states of the amino acids to a pH of 7.4. Induced fit docking was used to evaluate the interaction of compound 1 with PIM3 kinase. Figure 4 shows the top docked pose in the ATP binding pocket of PIM3. The main amino acids interacting with compound 1 is ARG125 and VAL54 (Figure 6A and B).

We also evaluated the interaction between compound 1 and DAPK1 (5AUT.pdb)¹⁶ using molecular modeling docking studies (Figure 6C and D). Since compound 1 activates/stimulates DAPK1, we posited that ATP would be in the ATP binding pocket and allosterically modulate it.¹⁷ Using MOE 2016 we docked ATP into the binding site of DAPK1 kinase similar to our previously published methods¹⁸. Using this model as our starting point, compound 1 was docked into the ATP binding pocket area with the OEDOCKING 3.2.0.3/FRED program as part of the OpenEye drug discovery suit (www.eyesopen.com). An advantage of using OEDOCKING/FRED¹⁹ is that a spatial box is delineated in which the compounds are docked. By extending the box around the ATP binding pocket of DAPK1 kinase which had the ATP bound to the model, we were able to find a docking solution that fits the hypothesis that compound 1 is able to allow for the ATP/kinase transition activity to occur in a more favorable state as compared to the kinase alone.¹⁸ As can be seen from this study, compound 1 is able to allow for an optimized positioning of the ATP for the gamma phosphate transfer to occur. This docking pose in part may explain the kinase activation by compound 1.

In contrast compound 1 did not inhibit or stimulate DAPK2. From our docking studies we found that compound 1 only weakly interacts with DAPK2 kinase (2YAA.PDB) via a hydrogen bond to the carboxylic acid group, and is lacking the interactions of the adenosine moiety to GLU94 and VAL96 as can be seen with ATP (Figure 7).²⁰ Additionally, there is a water network seen interacting with the phosphates of ATP (Figure 7). We posit that compound 1 is unable to bind to the pocket of ATP or orient itself to promote a stronger interaction for ATP with the kinase due to the waters in contrast to DAPK1. To our knowledge this is the first example of a small molecule which augments DAPK1 kinase activity.

Since several brain cancers such as from metastatic breast cancer are difficult to treat due to low brain distribution of the drug,²¹ we evaluated the permeability of compound 1 across an artificial barrier. The parallel artificial membrane permeability assay (PAMPA) is used in HTS screening which correlates to the permeability across the blood-brain barrier (BBB).²² In this 96 well micotiter plate assay compound 1 was added at 200 μM to the donor compartment containing phosphate buffered saline (PBS pH 7.4)/5% v/v DMSO and allowed to distribute across the hexadecane in hexane (5% v/v) organic layer on a filter plate to the acceptor compartment for 5 hours. The log_Pe was -3.735 suggesting that compound 1 may be able to move across the BBB. The efflux proteins such as p-glycoprotein (PGP) which part of the ABC cassette transporters play an important role in both brain distribution of a chemotherapeutic drugs as well as the accumulation of cancer drugs into tumor cells. We evaluated compound 1 for affinity for the PGP efflux transports in MDB-MB-231 breast cancer cells (Figure 8). This HTS assay follows the accumulation of the fluorescent Rhodamine 123 into the cells after the pre-treatment with the compounds for 2 hours. Fluorescence in the 96 well plates is determined with a BioTek Synergy 4 plate reader (Ex/Em 485/528). Figure 6 shows that compound 1, tested at 50 μM , does not affect the accumulation of Rhodamine 123 suggesting that compound 1 does not act as substrate for the PGP transporter. The voltage gated calcium channel blocker (VGCC) verapamil was used as positive control at 20 μM . These data suggest that compound 1 would not be actively transported from the cancer cells, and in the case of the BBB permeability would not be effluxed by PGP.

Phenotypical high content screens have the advantage of identifying compounds with drug-like pharmacokinetic properties (Distribution, metabolism and pharmacokinetics studies; DMPK) due to the involvement of organisms. In the case of the identified compound 1, we evaluated the serum albumin (SA) binding with the use of a bovine serum albumin (BSA) HTS screen. This HTS assay measures the quenching of the tryptophan in the BSA structure with Ex/Em 280/340 nm. As can be seen from figure 8 compound 1 has some affinity for serum albumin, with an IC₅₀ of 23.29 μM . This suggests that compound 1 will be able to have sufficient free fraction in the serum for pharmacodynamic interaction with the PIM3 kinase.

In conclusion, here we show the use of zebrafish embryos to identify a novel compound which can serve as lead for drug discovery campaigns. Compound 1 was able to inhibit PIM3 selectively and was found to activate DAPK1 kinase, which could prove to be a useful tool in drug discovery. This compound can be used as lead to develop novel anticancer

drugs. Future studies will be directed at increasing the selectivity of this lead compound for specificity towards Pim3 kinase inhibition or DAPK1 activation. Additionally, as neither kinase has been characterized in vertebrates, we also plan to develop better tools for dissecting the role of each of these kinases on the observed notochord and muscle deformation defect in zebrafish embryos.

Acknowledgments

The project described was supported by the National Institute Of General Medical Sciences, to WJG U54GM104942 and to LAH 1R01CA195727-01. The content is solely the responsibility of the authors and does not necessarily represent the official views of the NIH.

References

1. <https://www.cancer.gov/about-cancer/understanding/statistics>.
2. Buffery D. The 2015 Oncology Drug Pipeline: Innovation Drives the Race to Cure Cancer. *Am Health Drug Benefits*. 2015; 8:216–22. [PubMed: 26157543]
3. Liu H, Chen S, Huang K, Kim J, Mo H, Iovine R, Gendre J, Pascal P, Li Q, Sun Y, Dong Z, Arkin M, Guo S, Huang B. A High-Content Larval Zebrafish Brain Imaging Method for Small Molecule Drug Discovery. *PLoS One*. 2016; 11:e0164645. [PubMed: 27732643]
4. Faust K, Gehrke S, Yang Y, Yang L, Beal MF, Lu B. Neuroprotective effects of compounds with antioxidant and anti-inflammatory properties in a *Drosophila* model of Parkinson's disease. *BMC Neurosci*. 2009; 10:109. [PubMed: 19723328]
5. Oehlers SH, Flores MV, Hall CJ, Wang L, Ko DC, Crosier KE, Crosier PS. A whole animal chemical screen approach to identify modifiers of intestinal neutrophilic inflammation. *FEBS J*. 2017; 284:402–413. [PubMed: 27885812]
6. Geldenhuys WJ, Yonutas HM, Morris DL, Sullivan PG, Darvesh AS, Leeper TC. Identification of small molecules that bind to the mitochondrial protein mitoNEET. *Bioorg Med Chem Lett*. 2016; 26:5350–5353. [PubMed: 27687671]
7. Geldenhuys WJ, Caporoso J, Leeper TC, Lee YK, Lin L, Darvesh AS, Sadana P. Structure-activity and in vivo evaluation of a novel lipoprotein lipase (LPL) activator. *Bioorg Med Chem Lett*. 2017; 27:303–308. [PubMed: 27913180]
8. Blais JD, Chin KT, Zito E, Zhang Y, Heldman N, Harding HP, Fass D, Thorpe C, Ron D. A small molecule inhibitor of endoplasmic reticulum oxidation 1 (ERO1) with selectively reversible thiol reactivity. *J Biol Chem*. 2010; 285:20993–1003. [PubMed: 20442408]
9. Anreddy N, Hazlehurst LA. Targeting Intrinsic and Extrinsic Vulnerabilities for the Treatment of Multiple Myeloma. *J Cell Biochem*. 2017; 118:15–25. [PubMed: 27261328]
10. Zhang JH, Chung TD, Oldenburg KR. A Simple Statistical Parameter for Use in Evaluation and Validation of High Throughput Screening Assays. *J Biomol Screen*. 1999; 4:67–73. [PubMed: 10838414]
11. Wu P, Nielsen TE, Clausen MH. Small-molecule kinase inhibitors: an analysis of FDA-approved drugs. *Drug Discov Today*. 2016; 21:5–10. [PubMed: 26210956]
12. Wu P, Nielsen TE, Clausen MH. FDA-approved small-molecule kinase inhibitors. *Trends Pharmacol Sci*. 2015; 36:422–39. [PubMed: 25975227]
13. Shannan B, Watters A, Chen Q, Mollin S, Dorr M, Meggers E, Xu X, Gimotty PA, Perego M, Li L, Benci J, Krepler C, Brafford P, Zhang J, Wei Z, Zhang G, Liu Q, Yin X, Nathanson KL, Herlyn M, Vultur A. PIM kinases as therapeutic targets against advanced melanoma. *Oncotarget*. 2016; 7:54897–54912. [PubMed: 27448973]
14. Wang S, Shi X, Li H, Pang P, Pei L, Shen H, Lu Y. DAPK1 Signaling Pathways in Stroke: from Mechanisms to Therapies. *Mol Neurobiol*. 2016
15. Crystal Structure of the Human Pim1 in Complex with Ruthenium Organometallic Ligands. *To be published*

16. Yokoyama T, Kosaka Y, Mizuguchi M. Structural Insight into the Interactions between Death-Associated Protein Kinase 1 and Natural Flavonoids. *J Med Chem.* 2015; 58:7400–8. [PubMed: 26322379]
17. Simpson GL, Hughes JA, Washio Y, Bertrand SM. Direct small-molecule kinase activation: Novel approaches for a new era of drug discovery. *Curr Opin Drug Discov Devel.* 2009; 12:585–96.
18. Kumar V, Weng YC, Geldenhuis WJ, Wang D, Han X, Messing RO, Chou WH. Generation and characterization of ATP analog-specific protein kinase Cdelta. *J Biol Chem.* 2015; 290:1936–51. [PubMed: 25505183]
19. McGann M. FRED and HYBRID docking performance on standardized datasets. *J Comput Aided Mol Des.* 2012; 26:897–906. [PubMed: 22669221]
20. Patel AK, Yadav RP, Majava V, Kursula I, Kursula P. Structure of the dimeric autoinhibited conformation of DAPK2, a pro-apoptotic protein kinase. *J Mol Biol.* 2011; 409:369–83. [PubMed: 21497605]
21. Mittapalli RK, Adkins CE, Bohn KA, Mohammad AS, Lockman JA, Lockman PR. Quantitative Fluorescence Microscopy Measures Vascular Pore Size in Primary and Metastatic Brain Tumors. *Cancer Res.* 2017; 77:238–246. [PubMed: 27815391]
22. Geldenhuis WJ, Kochi A, Lin L, Sutariya V, Dluzen DE, Van der Schyf CJ, Lim MH. Methyl Yellow: A Potential Drug Scaffold for Parkinson's Disease. *Chembiochem.* 2014; 15:1591–1598.

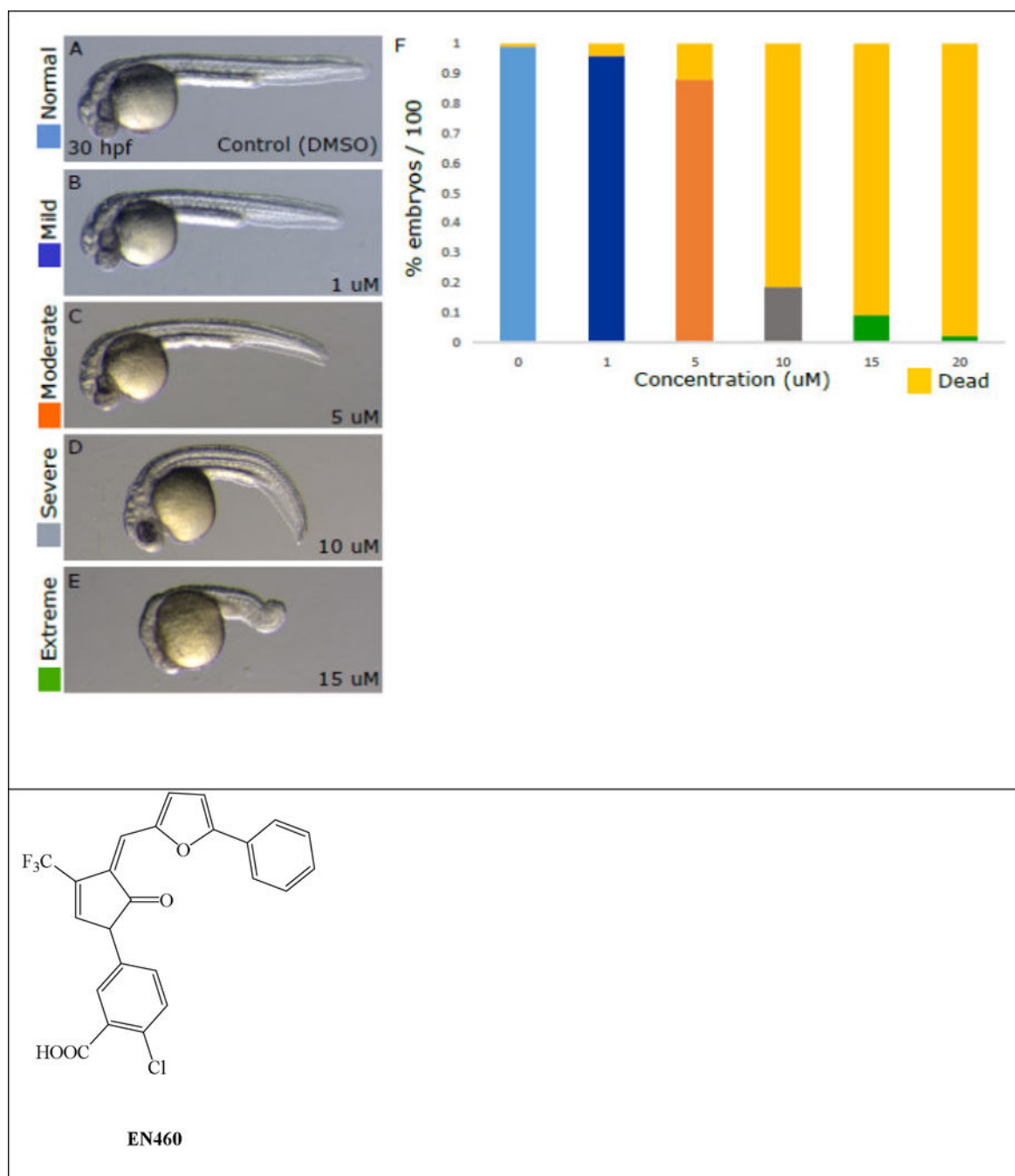


Figure 1.

Screening of the ERO1 inhibitor in zebrafish embryos. As can be seen, EN460 significantly affected the tail and notochord leading to an observable phenotypic change. At increasing concentrations of drug the morphological defects of the developing embryos became more and more severe. Defects were categorized according to degree of tail shortening and curvature (Mild to Severe) to effects on the entire embryo from head to tail (Extreme), A – E. Counts were normalized by treatment group to percentages of those embryos affected out of the total number treated. Treatment with 10 – 20 μ M dosages resulted largely in death of

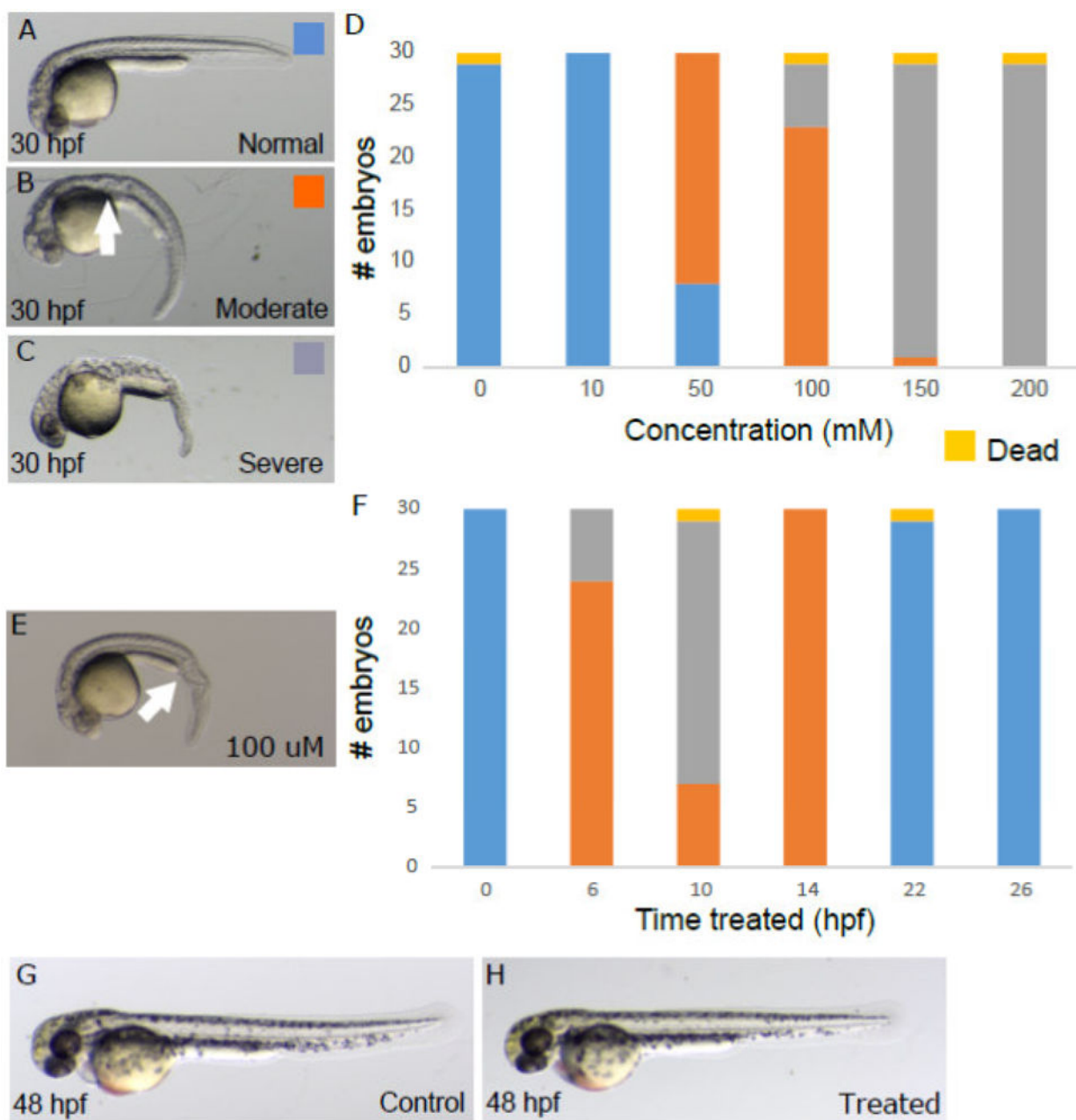
the embryos, F. The number of embryos treated with each dosage are: 0 μM control = 108, 1 μM = 48, 5 μM = 108, 10 μM = 108, 15 μM = 108, 20 μM = 48.

Author Manuscript

Author Manuscript

Author Manuscript

Author Manuscript



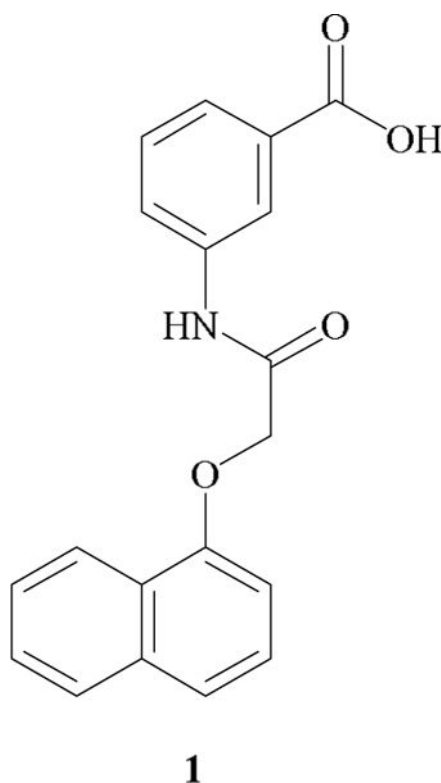


Figure 2.

High content screen identified compound 1. Zebrafish embryos were treated from 6–30 hpf in 12-well plates, $n = \sim 30$ embryos/group (A–C). Each well contained 1 mL of E3 media plus 1% DMSO with or without compound 1. At increasing concentrations of compound 1 the morphological defects of the developing embryos became more and more severe and were categorized based on severity of tail curvature with accompanying defects in somite and notochord development (Moderate and Severe). Death was hardly observed at even the highest compound 1 dosage of 200 μM (D). To determine the developmental window of time in which compound 1 causes these morphological defects we treated embryos with the 100 μM dose starting at different developmental time points until they were scored at 30 hpf (F). Using this methodology we determined that compound 1 targets a kinase between 6–14 hours of development when the notochord and somites are first forming as no defects were observed from treatment at this moderate dose after 14 hpf. We also observed that at the later treatment time of 14 hpf notochord and somite defects were localized more caudally compared to the earlier treatment time of 6 hpf (white arrows, B treatment starting at 6 hpf verses E treatment starting at 14 hpf). This suggests that the targeted kinase is active in different regions of the developing tail at distinct developmental time points, largely in newly forming body segments. G and H show examples of embryos treated from 30–48 hpf with 1% DMSO (control) or 1% DMSO plus compound 1 (treatment). At all dosages tried, embryos looked morphologically normal at this later treatment time.

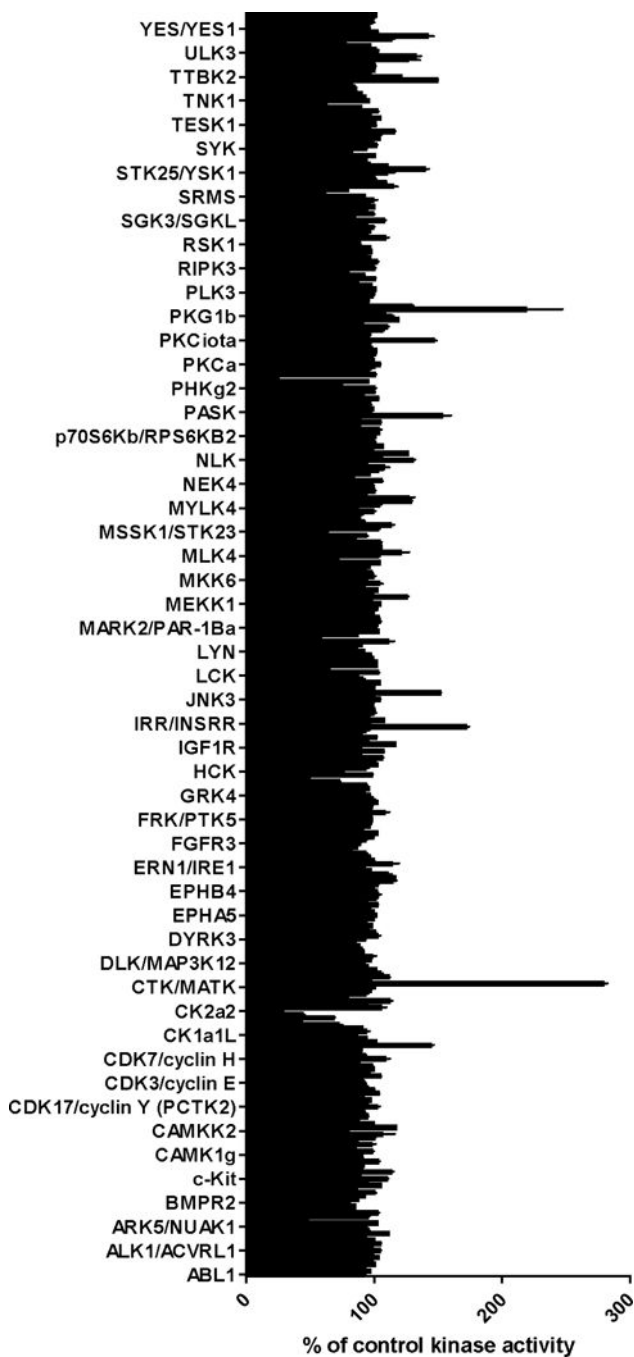
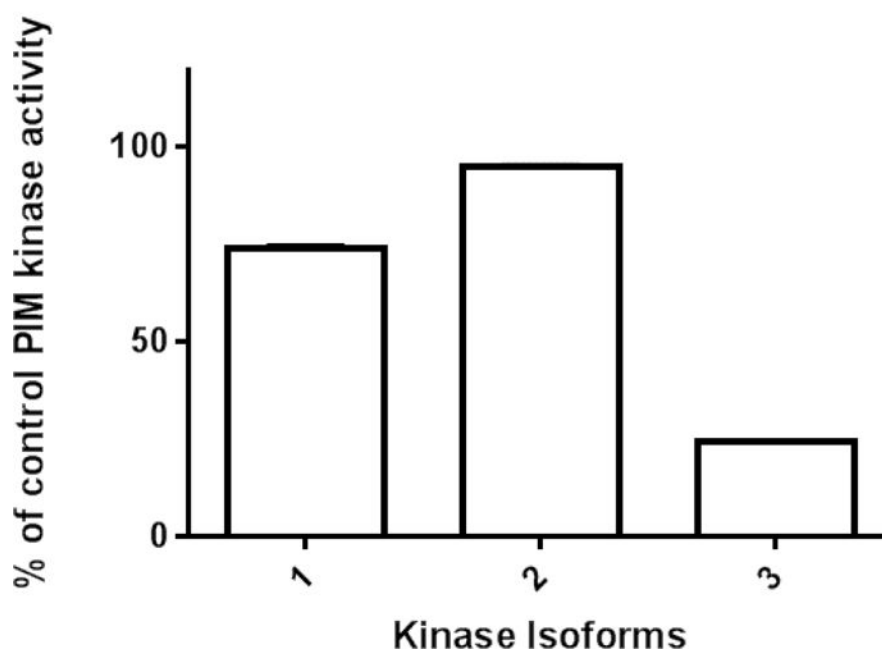
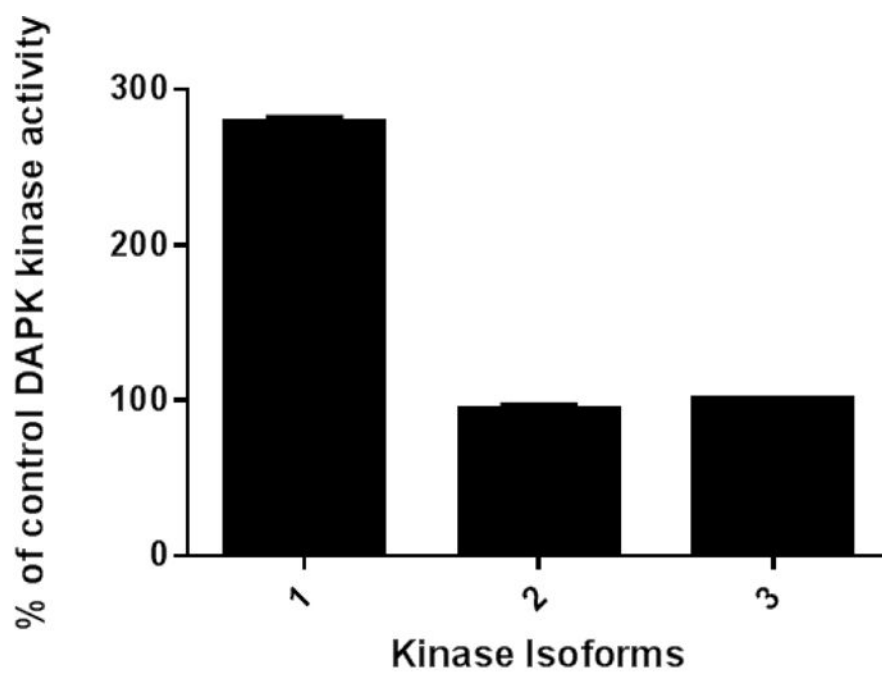


Figure 3. Kinase panel screen of 369 typical kinases with ATP as substrate. Compound 1 was tested at 10 μ M. The two kinases which were chosen from this screen were the PIM3 and DAPK1 as the two most extreme activities. N = 2.



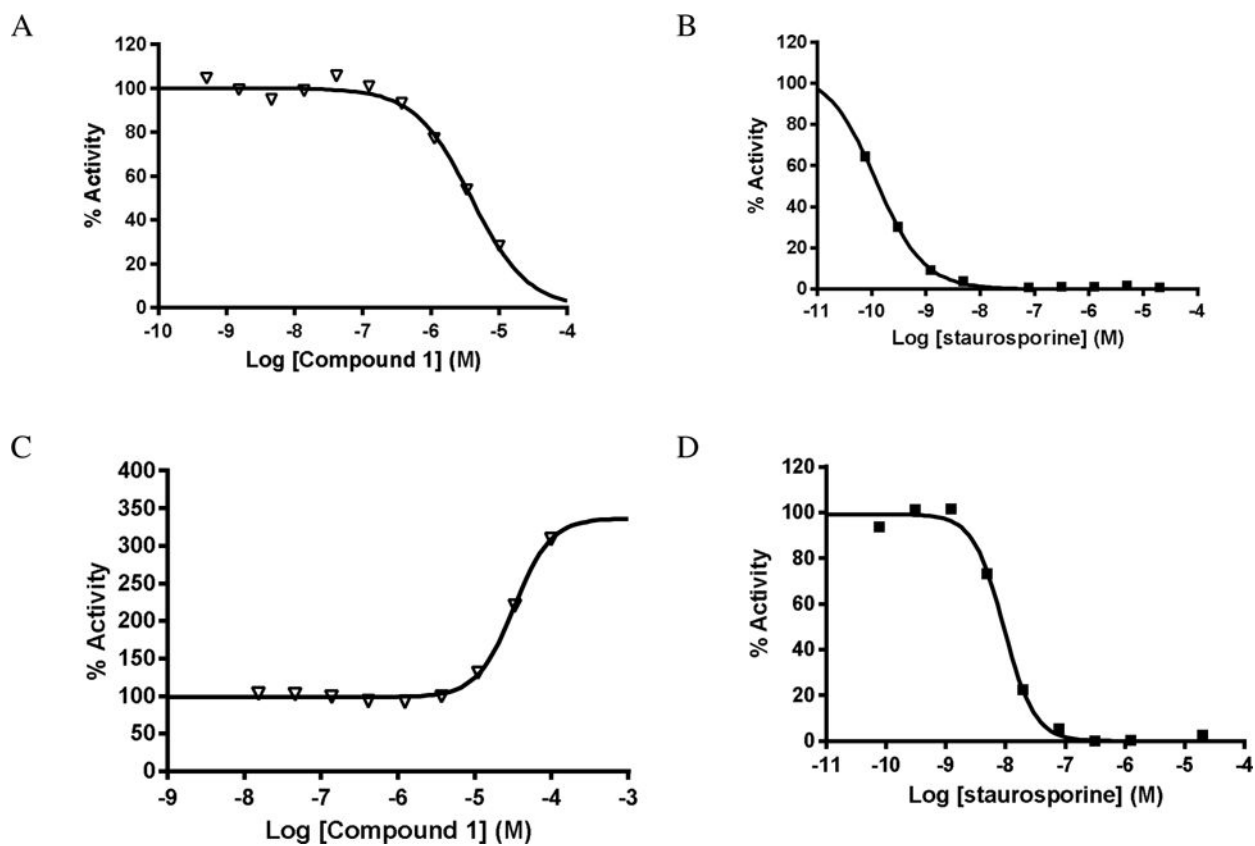


Figure 4. Compound 1 was found to inhibit PIM3 selectively, compared with PIM1 and PIM2 (A) and activate DAPK1 kinase, in contrast to DAPK2 and DAPK3 (C). Staurosporine was used as positive control for PIM3 (B) and DAPK1 (D). N = 2.

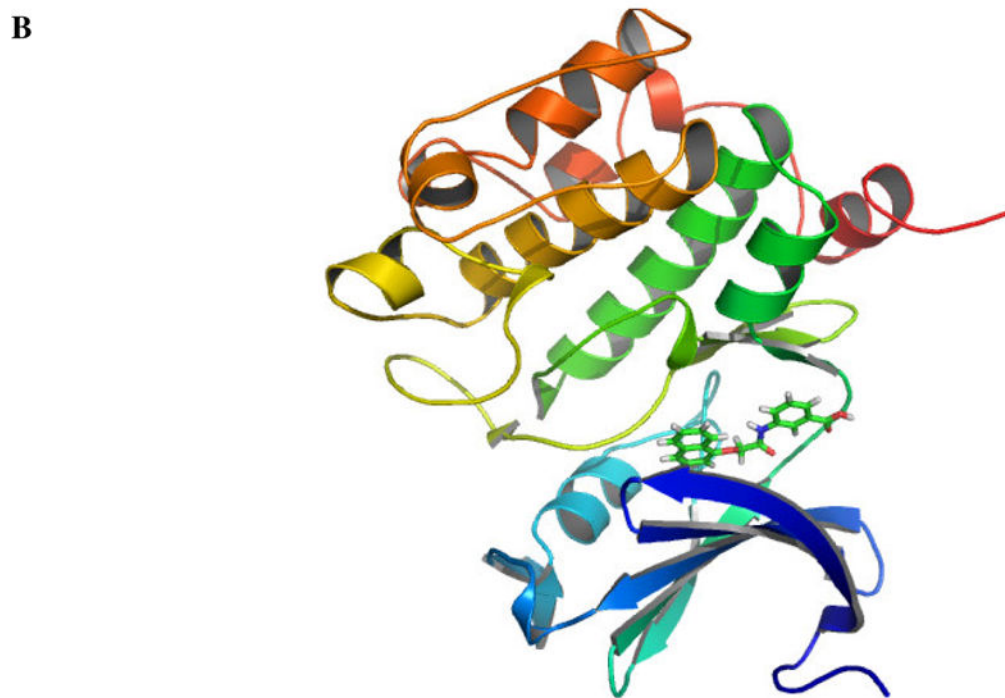


Figure 5. Structural alignment of the protein sequences of PIM3 and PIM1 for homology modeling (ClustalW alignment; A). The homology model of PIM3 was generated using YASARA software with PIM1 (2BZH) as structural template.

Author Manuscript Author Manuscript Author Manuscript Author Manuscript

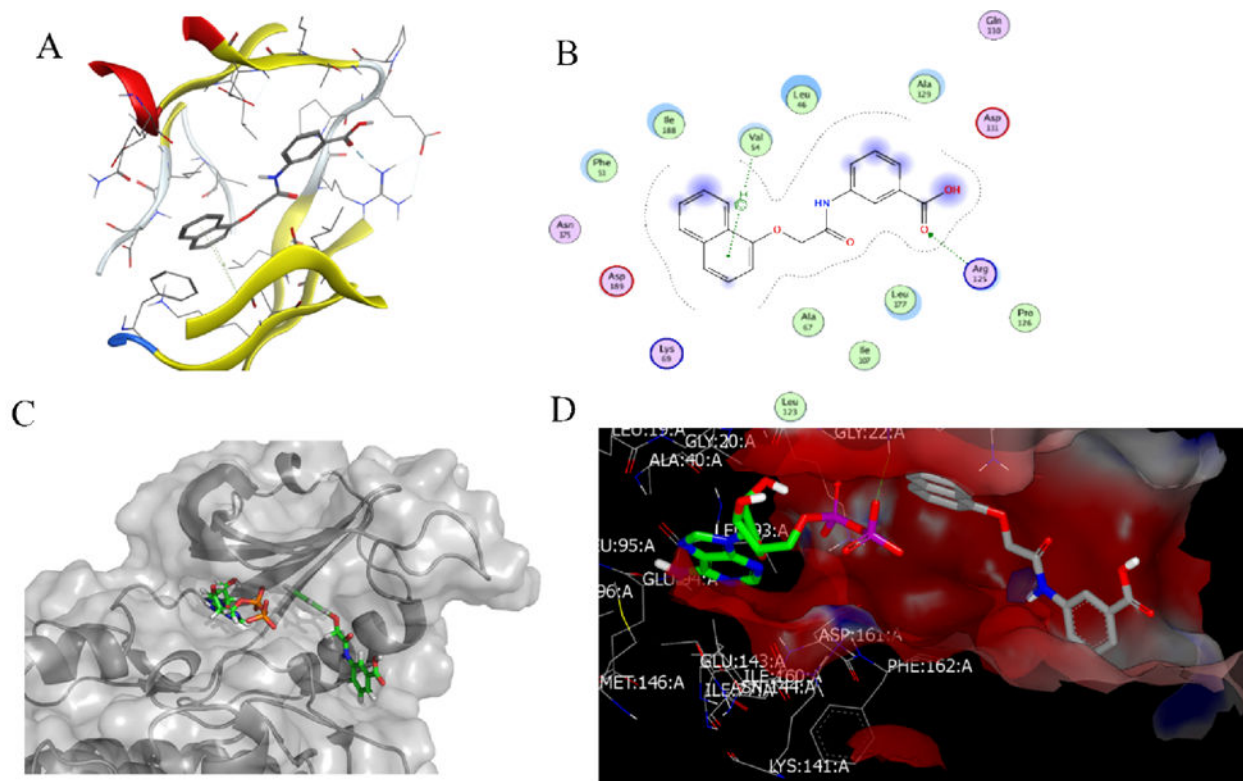


Figure 6. Compound 1 which was identified from the HCS in zebrafish embryos docked into the homology model of PIM3 (A) and the amino acid interactions (B). DAPK1 kinase activation is thought to occur via optimal orientation of the ATP for phosphorylation (C (Pymol) and D (VIDA)).

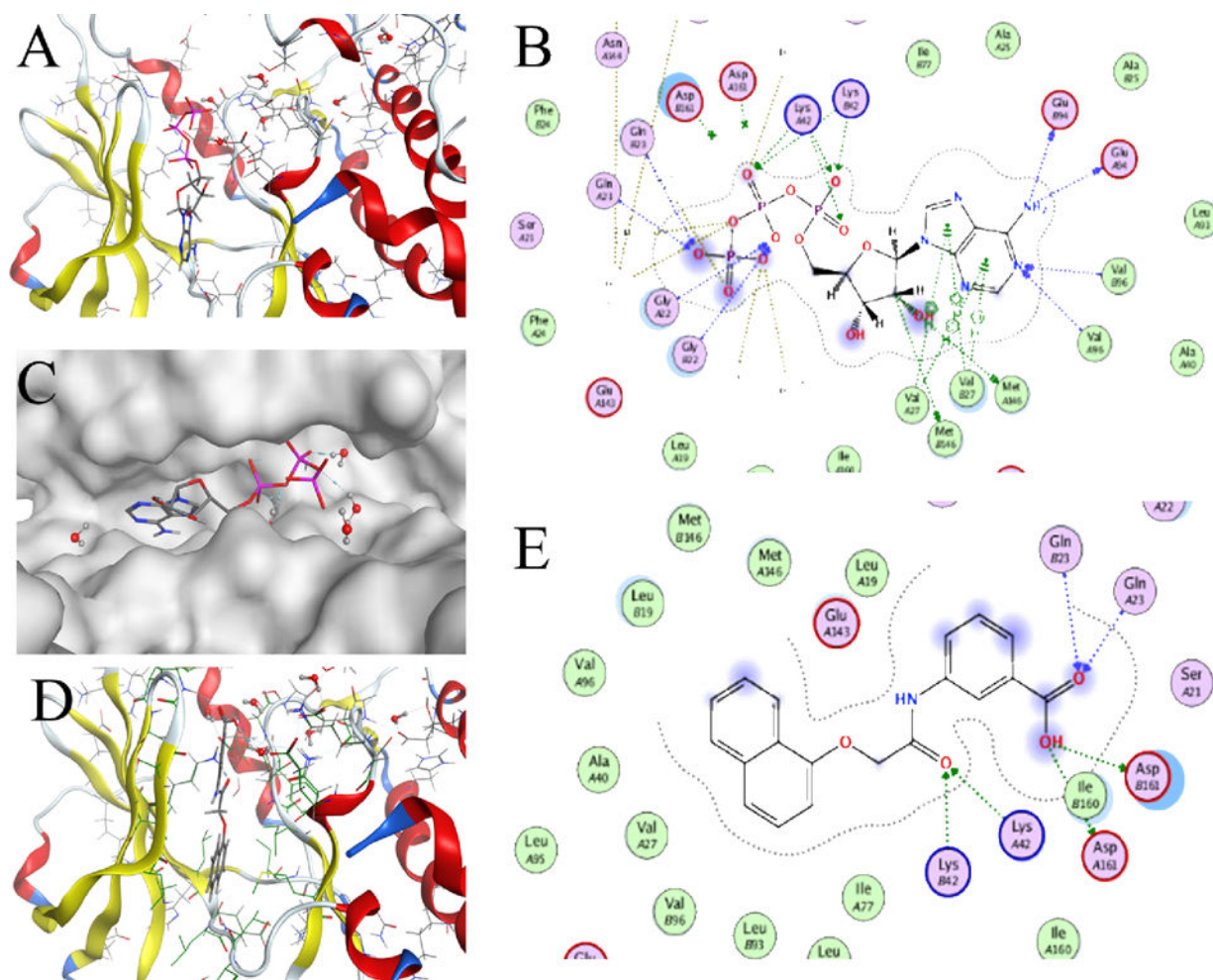


Figure 7.

Compound 1 interaction with the ATP binding pocket of DAPK2 (PDB: 2YAA). Compound 1 does not bind to DAPK2 via GLU94 and VAL96 as is seen with ATP (A and B), as well as the presence of a water bridge (C) prevents compound 1 from affecting the ATP phosphates (D and E) possibility as was suggested with the DAPK1 docking study.

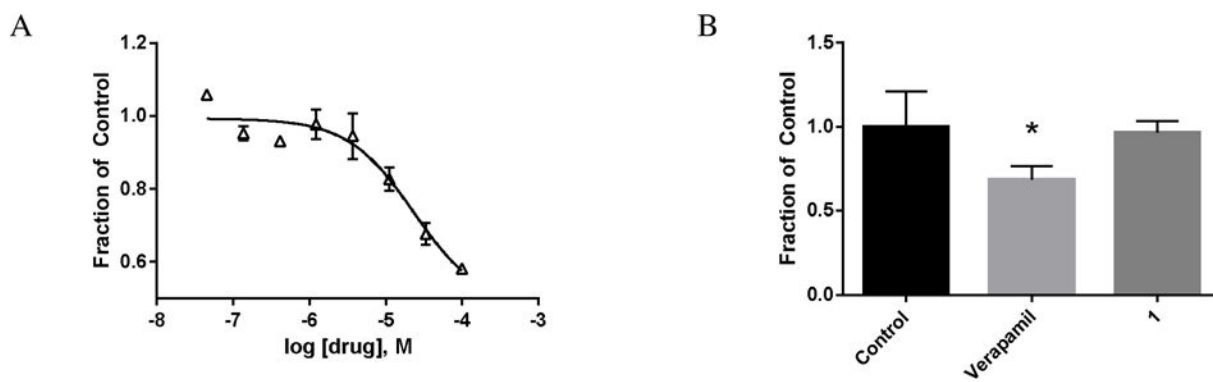


Figure 8. Compound 1 was evaluated in vitro for serum albumin binding (A) as well as affinity for the efflux transporter P-glycoprotein. * $P < 0.05$.